

## Research Article

# Performance Evaluation of a Bench-Top Precision Glass Molding Machine

**Peter Wachtel,<sup>1</sup> Peiman Mosaddegh,<sup>2</sup> Benn Gleason,<sup>1</sup>  
J. David Musgraves,<sup>1</sup> and Kathleen Richardson<sup>1</sup>**

<sup>1</sup> School of Materials Science & Engineering, COMSET, Clemson, SC 29634, USA

<sup>2</sup> Department of Mechanical Engineering, Clemson University, Clemson, SC 29634, USA

Correspondence should be addressed to Peter Wachtel; [wachtel@g.clemson.edu](mailto:wachtel@g.clemson.edu)

Received 14 September 2012; Revised 1 April 2013; Accepted 1 April 2013

Academic Editor: Essam Eldin Khalil

Copyright © 2013 Peter Wachtel et al. This is an open access article distributed under the Creative Commons Attribution License, which permits unrestricted use, distribution, and reproduction in any medium, provided the original work is properly cited.

A Dyna Technologies Inc. GP-5000HT precision glass molding machine has been found to be a capable tool for bridging the gap between research-level instruments and the higher volume production machines typically used in industry, providing a means to apply the results of rigorous instrumentation analysis performed in the lab to industrial PGM applications. The GP-5000HT's thermal and mechanical functionality is explained and characterized through the measurement baseline functionality and the associated error. These baseline measurements were used to determine the center thickness repeatability of pressed glass parts, which is the main metric used in industrial pressing settings. The baselines and the repeatability tests both confirmed the need for three warm-up pressing cycles before the press reaches a thermal steady state. The baselines used for pressing a 2 mm glass piece to a 1 mm target center thickness yielded an average center thickness of 1.001 mm and a standard deviation of thickness of 0.0055 mm for glass samples pressed over 3 consecutive days. The baseline tests were then used to deconvolve the sources of error of final pressed piece center thickness.

## 1. Introduction

The continual drive for advancing optical systems has led the optics industry towards extensive development of aspheric glass lenses. In many cases, the demand for aspherical optics has forced industry to evaluate a more cost effective process for the manufacturing of aspheric glass lenses over the labor and time intensive approach of conventional grinding and polishing. An emerging technology to handle the demand of aspherical lenses, called precision glass molding (PGM), is one in which the glass workpiece is heated and then molded into the desired lens geometry. Such processing requires significant understanding of mold and workpiece attributes, machine process parameters, and interactions at temperatures (viscosities) necessary to generate workpiece flow. A detailed understanding of the thermal and mechanical response of a given glass and mold material at elevated temperatures is not always available and is often realized by time-consuming iterative processes on expensive production

tools. A bench-top research platform to satisfy the needs of the user to control specific process parameters such as temperature, force, and position through the entire molding cycle in order to tailor the molding cycle to the desired glass has been commercially developed and evaluated. This paper discusses the use of such a tool, Dyna Technologies Inc.'s (DTI's) GP-5000HT, in support of material and process parameter optimization for the PGM process of visible optical glasses. The attributes and limitations of the as-purchased configuration are discussed along with the improvements made towards enhancing tool performance repeatability.

Moore Nanotechnology Systems, LLC [1] and Toshiba Machine Co. [2] sell commercial lens molding tools worldwide, and both have designed their machines to be compatible with medium to large volume production of optics, typically 5,000 and 30,000 pieces a year per machine, respectively. These machines are very similar in their flexibility of pressing parameters. They allow for force or position control. Depending on the motor, they can apply around

25 kN of force. Current industrial machines are offered with one of the following: resistive, induction, or infrared heaters. Infrared heaters have been found to be the most common. The temperature control is typically dictated by standard or manufacturer proportional, integral, and derivative (PID) feedback values [1–3].

Scientific research not aimed at realizing production volumes has a need for a smaller, bench-top sized version of such tools with flexibility in machine design, optical component geometries, molding atmospheres, heating geometries, and process parameters. The GP-5000HT precision glass molding machine from DTI [4] was designed and further modified at Clemson University for this purpose. The machine has functionality comparable to commercially available products but also the flexibility for laboratory testing, research and prototyping of various lens/mold designs, mold coatings, and lifetimes, and assessment of resulting part surface quality. Since its arrival at Clemson in the spring of 2010, the GP-5000HT has had two modifications made to it, to enhance the research functions of this machine. The first modification was the implementation of a high-temperature force transducer (Futek LCM200) to compensate the temperature effect on the force measurement. The second modification was the introduction of mold tooling inserts (the pieces which come into direct contact with the glass during molding) to allow the mold tooling shape to be easily changed with mold design changes or change in glass type. The present paper discusses results on only one glass type with a designated set of inserts, to illustrate tool function and performance, therefore, eliminating cross contamination of multiple glass types and enabling a further mold material/glass family interaction study. It should be noted that the modifications and associated changes employed have allowed the modified DTI tool to be used for studies conducted on both visible (oxide) optical glasses and infrared transparent (nonoxide, chalcogenide) glasses [5–7].

The main objective of the present study is to summarize the DTI tool's functionality and measure the accuracy of the new design's control over thickness of pressed or molded lenses. To this end, we have chosen part center thickness, CT, as an attribute which is critical in lens manufacturing as our metric. Measurement of CT in this context relates to the ability of the tool to repeatedly heat, press, and cool a lens blank (in this case a plano-plano part) under identical process parameters to assess resulting part uniformity. While not representative of the full capabilities of the DTI tool, CT assessment has allowed us to obtain statistically significant data on the influence of tool systems, in carrying out a simple press cycle on a commercially relevant optical material. To this end, mechanical, thermal, and pressed part repeatability tests were conducted using two polished planar tungsten carbide (WC) surfaces (mold inserts, Kennametal Inc., Latrobe, PA, USA) and L-BAL35 (Ohara Corp., Branchburg, NJ, USA) as the glass workpiece sample.

## 2. Machine Functionality and Baselines

The ultimate performance of the DTI press (referred to as the tool) is defined by the structural and thermal attributes

of the system and the ability of those components to return to a baseline condition in between pressing cycles. Thus, its ultimate functionality is a combination of the tool's structural and thermal response under defined molding cycle conditions and parameters. Knowledge of the baseline values of these attributes and how they vary/change with varying cycle times and "offline" cooling periods between presses dictates the cycle time possible for the tool. The GP-5000HT has a frame to house the heating system, mechanical system, and instrumentation. The frame is composed of two rectangular plates and four posts. The four posts close the structural loop of the machine by passing through the corners of the lower plate and connecting to the corners of the upper plate, so it has a closed frame structural loop. The components of the frame and other mechanical parts of the machine can be found in Figure 1. The machine systems described in this study are controlled by the limits and inputs of the press's instrumentation system. Simple thermal and mechanical baseline measurements were established to characterize the functionality of the press and determine possible sources of error during the glass molding process.

*2.1. Instrumentation.* The instruments used for assessing the press's performance are composed of sensors, measurement devices, and a controller. The sensors are used to send feedback to the controller enabling it to follow the command; they also act as safety features, preventing any damage to the heating system, mechanical system, or the user of the press.

The measurement devices for the tool include the thermocouples, pressure transducer, flow meter, load cell, and linear encoder used to govern the molding process. Holes aligned axially with the molds are used for inserting thermocouples to measure temperature and are located in the upper and lower molds up to 2 mm away from the back side of the mold tooling surfaces. This in turn places the thermocouples about 6 mm from the molded glass surface. The readings obtained from these thermocouples are used to estimate the temperature of the glass sample during the molding cycle. The outputs from these thermocouples are used as feedback for the heating elements. Two other thermocouples serve as safety sensors: one embedded in the wall of the molding chamber records the temperature within the molding chamber, while another is in the exhaust tube to monitor the exhaust gas temperature. The pressure transducer monitors the static pressure of one of the pneumatic lines coming into the molding chamber. The load cell is aligned axially with the molds, and it is connected in series to the actuator to instantaneously measure the force applied to the glass sample during molding. The linear encoder reads the displacement of the upper mold in respect to a home position. The home position is the furthest position from the bottom mold.

The signals from these sensors are sent to a Unitronics Vision570 Programming Logic Controller (PLC), which also serves as the human user interface (HUI) on the front of the press. There is Unitronics software that also allows the operator to run the press directly from a separate computer. The heating system has a separate software called EZ-Zone Configurator and is used to adjust the proportional, integral,

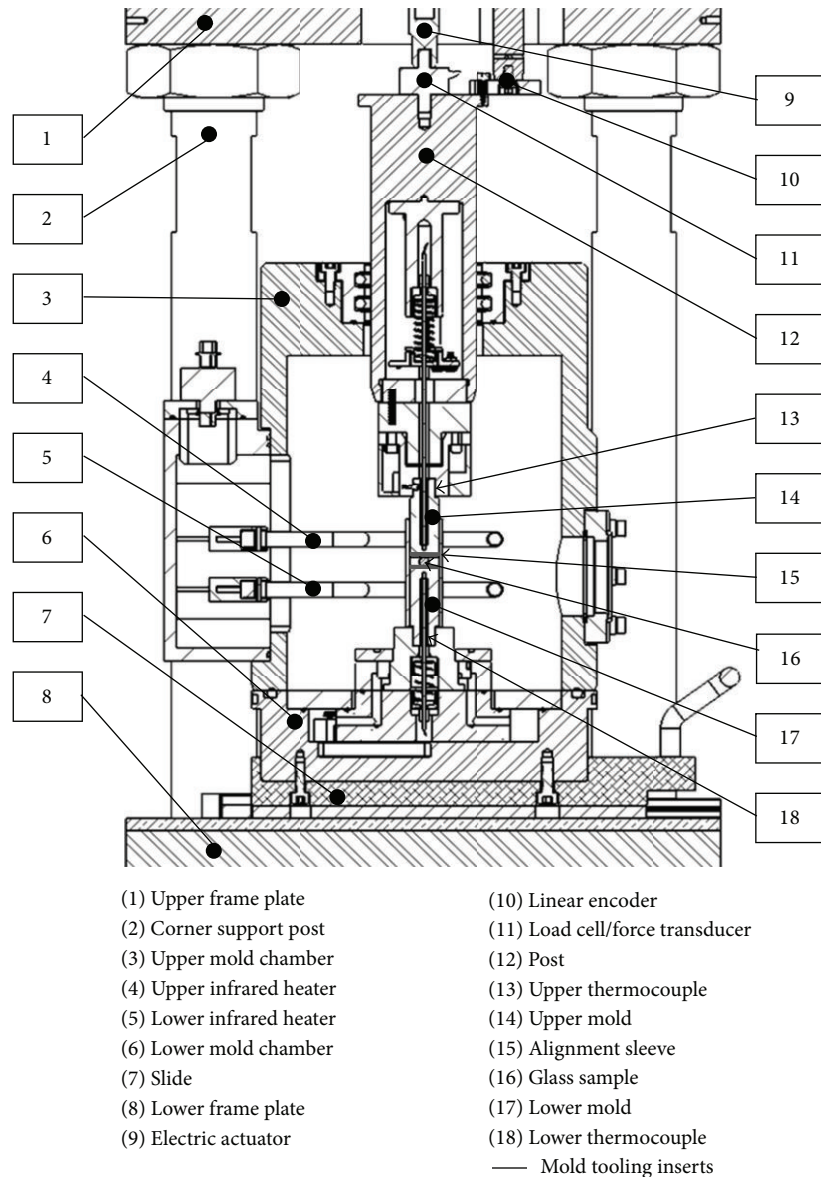


FIGURE 1: Cross-section of the GP-5000HT revealing its critical components. The pneumatic air cylinders that lift the upper mold chamber along with the control boxes, which contain the electrical equipment for operating the GP-5000HT, have been excluded.

and derivative (PID) values; this software needs to be run from a separate computer because the PLC and the EZ-Zone software cannot both be connected at the same time as the inputs to heating system will interfere. The PLC stores memory on either the hard memory of the PLC or an SD card.

**2.2. Mechanical Systems.** The mechanical system is composed of an electric actuator and two pneumatic cylinders attached to the upper frame plate. The pneumatic cylinders are used to raise and lower the upper molding chamber. The upper portion of the molding chamber is connected to the ends of the pneumatic cylinders, and the lower portion is attached to slide rails on the lower frame plate. This allows the lower portion of the molding chamber to slide in and out from

under the upper molding chamber. A back stop (set screw) on the slide rails aligns the lower molding chamber with the upper. The back stop is fitted with a sensor that activates when the lower molding chamber is resting against it allowing the upper molding chamber to be moved. The electric actuator is also linked to this sensor but can be disabled in the manual control mode.

The electric actuator provides the movement and force along the axis of the molds needed for molding the glass. The actuator is mounted to the upper frame plate and is connected in series with the load cell, the support post (post), upper mold, and upper mold tooling, respectively. The support post goes through a seal housing that is on the upper molding chamber so that the molding chamber is not disrupted by ambient air. The mold inserts/tooling are

the only objects in the system that are in contact with the glass during the pressing cycle. The upper and lower mold tooling is approximately 4 mm in thickness and sit between their corresponding mold face and the glass. The mold tooling is used indirectly to monitor mold/glass interactions by measuring the change in tooling surface roughness as a function of cycle number, which after multiple cycles changes as nanoscale deposits of glass are formed or mold tooling material pulls out of the mold tooling. The use of multiple small tooling inserts can decrease contamination and allows increased flexibility of molded shapes. The lower mold and mold tooling remain stationary throughout the molding process and are mechanically connected to the lower molding chamber. A sleeve around the lower mold and mold tooling is utilized to align the upper and lower molds which are made of tungsten carbide (WC). The WC is used because of its robust mechanical and thermal properties at higher temperatures [8]. Alternative mold/insert materials can be employed as needed for the desired glass type/heating method/temperature range; however, the present work only describes finding for WC with L-BAL35 glass.

A preliminary set of baseline measurements were performed at room temperature in order to characterize the repeatability of the mechanical structural response and how these components settle under force over a number of pressing cycles. These baseline measurements define the position and the repeatability of the bottom mold position at room temperature because that position is used as a reference to determine the glass workpiece thickness during the molding cycle. A number of experiments were performed in order to determine the exact position where the molds are in contact. From one molding cycle to the next, there are four steps to loading the sample. The four steps involve putting the alignment sleeve in place, putting the bottom insert in place, inserting the workpiece sample, putting the top mold insert in place, and sliding the bottom mold housing directly under the upper mold housing. Experiments were conducted with each of these steps to understand sources of error in the position read-out. The bottom mold position repeatability experiments were conducted by bringing the upper tooling down until it reached an 88 N force, and the position was recorded; this load level was selected because it is a low force that would be able to overcome internal friction of the system during the pressing cycle. This procedure was repeated 10 times for the purpose of statistical analysis and the resulting bottom position recorded. Due to bottom position being a physical starting point for the measurement of the system, the range of the bottom position will directly correlate to the error of the final pressed part CT. Table 1 lists the total range in the bottom position measured for each experiment and a percentage of that range given by the standard deviation of the experiment. Another metric monitored during this test was the change in system friction by recording the load under movement before the upper mold came in contact with the bottom or the sample. This is important because a change in force would mean that the upper mold tooling was coming in contact with the sleeve and would then create extra stresses in the system, false force readings, bending moments, and wedging of the sample. Change of system friction can be seen

by a change in the system's static force when the mold tooling was above the sleeve and in the sleeve.

Table 1 shows that the deviation in the bottom position remains smaller than  $1\ \mu\text{m}$ , which is the GP5000HT's LVDT position sensitivity, until experiment 4. The deviation increases in experiment 4 and increases even more in experiment 5. Experiment 5's procedure is identical to that used for inserting the glass molding preform during an industrial pressing cycle. This result indicates that a part of the deviation in final pressed part center thickness comes from the sample placement in the molding cavity and from the total movement of the bottom mold housing. Another observation from this test is that the static force did not increase, which means the friction of the mold tooling movement did not change with the addition of the pieces required for molding.

**2.3. Heating System.** The press has two different types of heat sources that can be employed, depending on the pressing process under consideration; one set uses resistive heaters and the other infrared (IR) heaters. The resistive heater setup uses resistive coils that surround and are in contact with the molding sleeve. Using the resistive heaters, the press is designed to reach temperatures of  $600^\circ\text{C}$ . The IR heater setup uses two omega-shaped IR lamps that circle and do not touch the sleeve and are connected to the upper mold chamber. The IR lamps have a reflector on the outer half to help reflect more light towards the sleeve. In addition to the reflectors on the lamps, reflective foil is placed by DTI on inner surfaces of the chamber to improve the fraction of light reflected back to the sleeve and keep chamber parts from overheating.

The heating system uses two separate heating elements, an upper and a lower, to increase temperature uniformity. Uniform temperature control becomes important if the glass being pressed has a steep viscosity curve (where the viscosity changes drastically as a function of temperature) because a temperature gradient could cause unfavorable, nonuniform glass flow. The temperature uniformity is especially important for PGM process during the pressing and the cooling sections of the pressing cycle, and not as important in the heating and soaking sections, as the glass and the system are still reaching equilibrium and less than ten percent of the total pressed part deformation should be taking place (see Figure 7 for a schematic of the PGM force and temperature profiles showing these sections).

The feedback loop controlling the heaters is based on two thermocouples embedded in the upper and lower molds roughly 6 mm from the molding surface, and the thermocouple output feeds back for the corresponding upper or lower heater. The heaters are controlled through one of two approaches, an open-loop control and a closed-loop control. The closed loop is controlled by a proportional, integral, and derivative (PID) feedback loop in the PLC and is activated by the feedback from the thermocouples. The PID values can be adjusted to increase the variability of the temperature control with separate software to control the system. Different temperature settings in a program will be optimized with different PID values and can be determined with an autotune function. The autotune has three different settings: over,



TABLE 1: Results of the bottom position repeatability experiments.

	Experiment 1	Experiment 2	Experiment 3	Experiment 4	Experiment 5
With sleeve	No	Yes	Yes	Yes	Yes
With mold inserts	No	No	Yes	Yes	Yes
With sample	No	No	No	Yes	Yes
With full movement	No	No	No	No	Yes
Total bottom position range ( $\mu\text{m}$ )	1	0	0	5	6
Bottom position standard deviation ( $\mu\text{m}$ )	0.5	0	0	1.7	1.8
Change in static force (N)	N.A.	0	0	0	0

under, and critical, which allow for slightly different tunability for the heating of the system to temperature; the three autotune settings react differently at different temperatures, and the response needs to be experimentally determined for each new thermal and material profile used. For even more advanced control of the heaters, the PID values can be changed manually. The IR and resistive heaters respond differently to the autotune function as shown in Figure 2. Figure 2 shows that the IR lamps heat up faster than the resistive heaters. The IR heaters are the heating devices the machine is designed for as the instrument is designed to operate at temperatures up to  $800^\circ\text{C}$ . The IR heaters also hold temperature better than the resistive heaters as shown in the reduced modulation seen in the temperature variation with time data depicted in the inset of Figure 2.

In the second method of control, the open loop, the ability to manually set the heater power is accessible; however, there is no feedback from the thermocouple. The open-loop control is valuable as a tool for adjusting the gain or power going to the heaters. This ability is important to permit heater power optimization and in turn can allow higher operating temperatures and higher heating rates. If higher operating temperatures and faster heating rates are not necessary for the desired pressing application, the gain can be adjusted down accordingly to preserve the life of the IR lamps. With the current gain settings on the controller at about 90% of the allowed gain for the heaters, the 100%-power heating rate can be realized as is shown in Figure 3. A simple exponential decay has been used to fit the data as can be assumed based on heat transfer considerations [9].

Optimization of the PID values has led to a temperature control during the pressing section of the molding cycle of  $\pm 1^\circ\text{C}$  of the commanded temperature for the two different heating elements. The IR lamps attained this level of control directly from an autotune; however, the resistive heater setup needed further adjustment after the autotune by manually changing the PID values in order to reach that level of control.

The same PID values used for the heating cycle are also used for the cooling cycle. Inert gas, typically unfiltered, reagent-grade nitrogen, is used to cool the press from operating temperature to  $150^\circ\text{C}$ . This temperature, if below the workpiece's glass transition temperature, is deemed a safe temperature to open the system housing/sleeve. The cooling limitations are based on the fastest cooling provided by maximum nitrogen flow in the system at a given temperature. Figure 3 also depicts the measured cooling rate data with

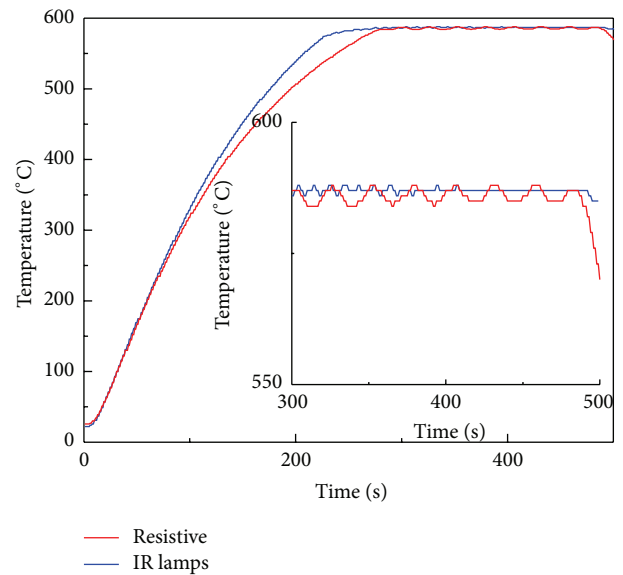


FIGURE 2: The difference in resistive and IR heaters during the heating and pressing stages of a molding cycle after the autotune.

curve fit for the maximum gas flow. The curve fit to the data is simple exponential demonstrating basic heat transfer with Newton's law of cooling. Newton's law of cooling does not fit the data exactly because the system components are at different temperatures at the start of the cooling cycle and the total cooling rate will be a distribution of cooling curves.

The IR heaters have demonstrated superior thermal stability; they will be the heating elements used for the remainder of the present study. The heating system causes thermal expansion of the press components when at molding temperatures, which can have a dramatic impact on the resulting pressed piece thickness if not properly accounted for. An evaluation of the system thermal expansion is performed with the experimental settings of experiment 5 from Table 1. The sample used was fused silica, with a glass transition temperature above  $900^\circ\text{C}$ , it does not compress or flow at the temperatures studied, and the thermal expansion of the silica is negligible compared to that of the rest of the system. The tests were conducted by finding the bottom position and holding an 88 N force at room temperature as defined in the baseline section above and then bringing the furnace up to temperature while recording the change in

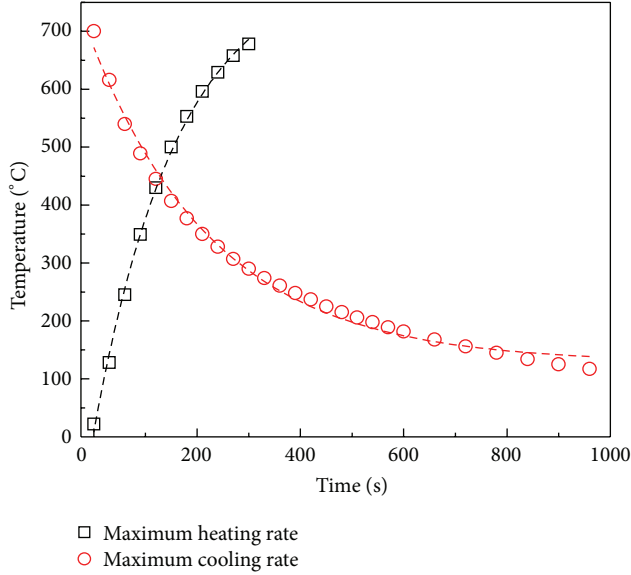


FIGURE 3: Data from temperature response, as measured by the average of the mold tooling thermocouples, from the IR lamps on full power fitted with a simple exponential decay to the data (squares, heating); and the maximum cooling of the system with a simple exponential decay fit (circles).

bottom position to assess and quantify the overall system thermal expansion. An example of the results of a single test is shown in Figures 4(a) and 4(b), the thermal expansion was measured at specific times at different temperatures across multiple consecutive cycles.

It should be noted that this test does not give a method for finding the bottom position at temperature. This is because of the large thermal mass of the press which prevents the system from returning to room temperature before the next pressing cycle. The time for the press to reach room temperature can be over eight hours; this is not a practical time scale for producing lenses. To understand the effect of the tool's thermal mass on the systems thermal expansion, an extended thermal expansion study has been made by recording the bottom position at the end of the pressing cycle for seven consecutive cycles. These results are shown in Figure 4(b). Knowing the position accurately is important in precise control of the PGM process because transitions between stages in the molding cycle (depicted later in Figure 7) are position limited. For example, only when the press reaches the final, user defined press position, it ends the pressing stage of the molding cycle and begins the cooling stage. Analysis of the final press position as a function of molding time and temperature is done by ramping the heating elements at the maximum ramp rate to 300, 500, or 700°C and holding for 120, 600, or 900 seconds. These temperatures were chosen as temperatures close to those of chalcogenide lower molding temperatures and oxide higher molding temperatures, effectively representing the full planned temperature range of the press. The 120-second and 600-second soaking times were chosen because they are the typical limits of time at temperature for industry; the 900-second time was chosen as a time that

allows the system to get closer to true thermal equilibrium. Each combination of the time/temperature parameters was run for seven consecutive molding cycles. The extremity results, the highest and lowest temperatures, with the shortest and longest hold times, of this test are shown in Figure 4(b). These results demonstrate that the thermal mass of the system does not reach an equilibrium state until the third or fourth consecutive molding cycle, therefore, demonstrating the need for warm-up cycles to bring the system into a “steady-state” following initial power on first thing in the day. The steady state region, where the thermal expansion is essentially constant with subsequent pressing cycles, begins at cycle number four for each of the different expansion runs tested. This figure shows that the final pressing position is greatly affected by the thermal expansion of the system, which at higher molding temperatures can be greater than 1,200  $\mu\text{m}$ . Figure 4(b) also shows that the final position set point will be a function of the time at temperature, due to the large thermal mass of the system. This experiment demonstrates why it is not currently possible in industry to predict the exact final press position without doing iterative pressing cycles and changing the final position, a trial-and-error type solution that our work seeks to minimize. The results of the measurement of the deviation in bottom position for the varying temperature and time regimes shown in Figure 4(b) were analyzed to quantify the magnitude of this variation, and the resulting deviation data are summarized in Table 2.

Table 2 indicates that the error in the final press position is neither a function of temperature nor of the duration of time at temperature. Therefore, the error could be from the nonequilibrium thermal state of the system; the heater power is still pulsing when trying to hold a molding temperature. These thermal expansion measurements show that the average error in the press position when using a molding temperature above 300°C is up to  $\pm 3 \mu\text{m}$ . The final positions measured in these tests were used to generate a predictive final position set point expression as a function of temperature and time at temperature. All fits for the baseline thermal expansion were calculated using a first-order exponential decay function following Newton's first law of cooling; the first-order exponential is needed because the system does not fully reach equilibrium. The baseline function is comprised of a first-order exponential decay function as a function of time where each fitting parameter is then an exponential decay function of temperature. The full thermal expansion baseline function to predict the final press position ( $FPP_E$ ) in  $\mu\text{m}$  is given below:

$$FPP_E = \left[ A_1 e^{(-T_m/B_1)} + C_1 \right] \left[ e^{-t/(A_2 e^{(-T_m/B_2)} + C_2)} \right] + \left[ A_3 e^{(-T_m/B_3)} + C_3 \right], \quad (1)$$

where  $T_m$  is the molding temperature in °C and  $t$  is the time in seconds. The fitting parameters are given in Table 3.

Due to the exponential nature of the fit, care needs to be taken in the fitting process to not disregard significant figures. The model fit with two less significant figures overestimates the fit by 10  $\mu\text{m}$  at high temperature and time. The  $FPP_E$  fitting parameters in (1) at a molding temperature of 566°C

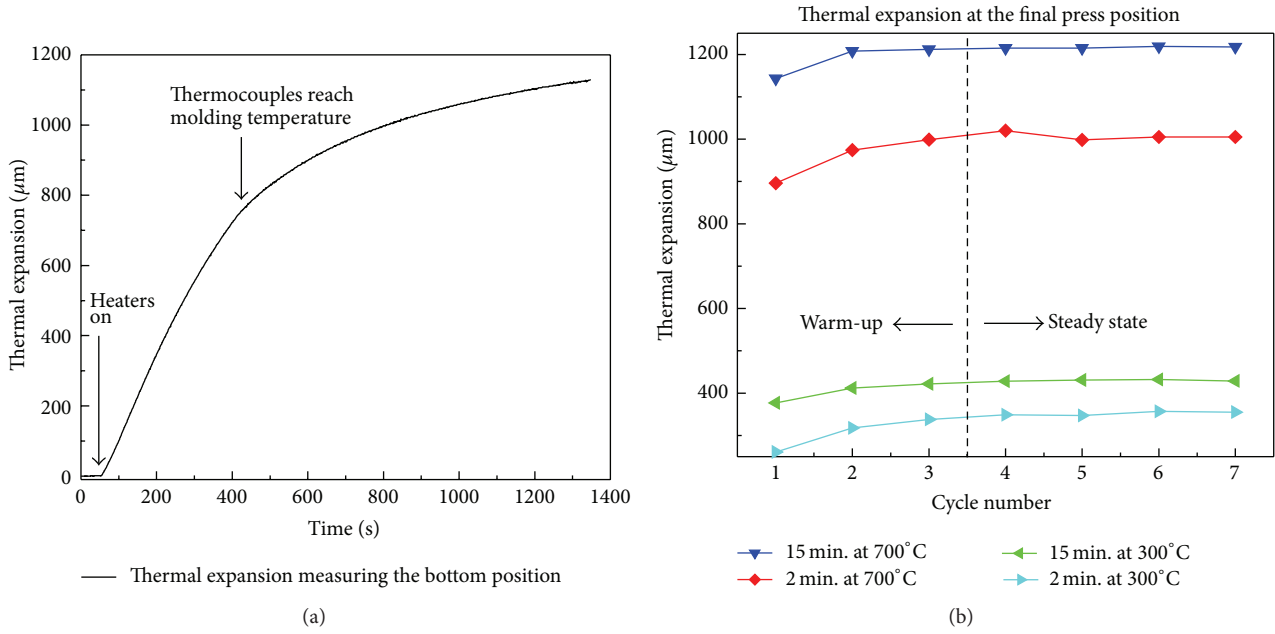


FIGURE 4: (a) A typical thermal expansion of the system, measuring the bottom position change in the press as a function of temperature. (b) The trend of the bottom position measurement at defined times and temperature for seven consecutive cycles.

TABLE 2: Deviations in the final press position for the test shown in Figure 4(b).

Temperature ( $^{\circ}\text{C}$ )	300			500			700		
Time (s)	120	600	900	120	600	900	120	600	900
Thermal Expansion ( $\mu\text{m}$ )	$277 \pm 2$	$372 \pm 4$	$376 \pm 2$	$534 \pm 3$	$663 \pm 2$	$694 \pm 4$	$848 \pm 1$	$1018 \pm 1$	$1090 \pm 3$

TABLE 3: Fitting parameters for the  $\text{FPP}_E$  in (1).

	A	B	C
1	-0.07425	-85.05	-225.47
2	61.90	-246.84	-65.13
3	243.00	-394.21	-145.04

with a soak time of 300 seconds were tested for model validation. The model predicts an expansion of  $711 \mu\text{m}$ , and the experimental value was measured to be  $710 \pm 2 \mu\text{m}$ , matching the predicted model value fit within the experimental values and system error. It should be noted that the thermal mass affected by a given molding cycle changes with temperature until the molding temperature is above  $300^{\circ}\text{C}$  due to the nonsymmetric geometry of the system. This effect causes the  $\text{FPP}_E$  baseline to be valid only above  $300^{\circ}\text{C}$ . More evidence of the nonsymmetric nature of the tool's thermal mass impacting results below a  $300^{\circ}\text{C}$  molding temperature can be seen in the structural stiffness measurements of the machine discussed below.

**2.4. Structural Stiffness of the Machine.** The theoretical stiffness of the machine including upper plate, corner posts, and lower plate is designed and stated by the manufacturer

to be  $351 \text{ MN/m}$  meaning that the theoretical deflection is expected to be approximately 2.85 micrometers at a force of 1 kN.

To experimentally evaluate the machine structural stiffness at room temperature and elevated temperatures, the linear drift of the force transducer was measured using a shunt calibrator to both calibrate and monitor the force during testing. The shunt is attached to the force transducers circuitry where it is not affected by heat, and the effect of the force transducers internal circuitry was then monitored as a function of molding temperature. The shunt calibration showed a linear output from the force transducer as a function of increasing temperature up to  $800^{\circ}\text{C}$ , indicating that the transducer was within its working temperature range during the subsequent tests. The linear drift of force as a function of molding temperature determined from the temperature dependence of the shunt test is roughly given by

$$F_a = F_r - (0.045T_m), \quad (2)$$

where  $F_a$  is the actual force in Newtons when  $F_r$  is the machine's recorded force in Newtons and  $T_m$  is equal to the molding temperature in degrees Celsius. The correction factor of 0.045, determined from the shunt test, has units of Newtons per degree Celsius and indicates that the forces change by 4.5 N per  $100^{\circ}\text{C}$ .

With the force correction as a function of temperature known, systems structural stiffness as a function of temperature can be measured. The structural stiffness of the instrument is determined by measuring the press position as a function of applied force. The structural stiffness experiments were performed at room temperature, 300, 500, and 700°C in order to cover the usable temperature range of the press. The tests were conducted by bringing the press to the target temperature and soaking for a minimum of one hour, then bringing the mold tooling in contact with a silica sample, and applying a predetermined force. The bottom position was measured at an 89 N force before and after all of the experiments to ensure that the system was at equilibrium. The test was conducted by allowing the press to control the movement of the mold tooling while reaching a set force up to 890 N and also by manually moving the actuator and measuring the force the press records once the actuator is stationary. The two methods of obtaining data were to determine if the machine could record a dynamic effect to the structural stiffness. If the output from the DTI for the position or the force was at different rates or one lagged behind another, the structural stiffness would be skewed higher or lower depending on which one lagged behind. If there was a lag, the data would also seem to be a function of actuator speed. The data between the two recording methods did not show any significant difference in results, and the data was combined to create a larger data set for determining the structural stiffness. A graphical example of a single data set is shown in Figure 5(a).

The raw position output data has been zeroed at furthest point of the actuator from the bottom mold, so as the top mold comes closer to the bottom mold, the raw data shows an increase in position. It is clear that the molds come into contact at a position of 15.439 mm. Figure 5(b) shows the calculation of the structural stiffness of the instrument through the application of a linear fit to the change in force as a function of position (the red line). As expected, as the position is increased (i.e., the molds are forced into contact) the force measured by the system increases linearly, and the slope of this line is the structural stiffness.

The first step in analyzing the raw data was to isolate the values after the first contact was made with the mold tooling and when force is initially applied. To complete this, all of the data with a force of 22 N or less was discarded. Furthermore, a linear fit of the data will minimize the deviation of the data in the  $y$  variable only, and due to the large scatter in the  $x$  variable values, the fit does not minimize the total deviation of the data. To correct this directional discrepancy for a linear fit, the force values over every 22 N were averaged, and the fit was performed using the averaged points. An example of the 22 N bin average plot and the linear fit is seen in Figure 5(b). By creating 22 N bins and taking the average, the deviation in the position is minimized, and the fit will minimize the deviation in the force. As seen in Figure 5, there is a very clear linear trend, and the fit has an  $R^2$  value of 0.8 which is quite good for such a large data set.

This process of data reduction was used for all of the temperatures studied. The slope of the linear fit in Figure 5(b)

is the structural stiffness, and the slopes across all of the temperatures can then be plotted as a function of temperature. Figure 6 shows the structural stiffness of the GP5000-HT as a function of temperature.

The measured structural stiffness at room temperature is 125 (MN/m) and is almost one third the theoretical value of the machine's frame stiffness of 351 (MN/m). This drop in measured stiffness can be attributed to the many mechanical connections and joints in the axis of the molds and the structural loop connecting to the frame.

Figure 6 shows that the structural stiffness decreases with increasing temperature, which is the expected trend. From room temperature to the highest operating temperature, the structural stiffness of the machine decreases by 32%. At the actuator's maximum load of 2.2 kN, the compression of the system measured by the LVDT can vary by 10  $\mu$ m. The stiffness is not a linear function of temperature in this system because the heat transfer and the thermal mass are not symmetric and change as function of temperature. Although the structural stiffness does not have a perfectly linear dependence across all temperatures, due to the change in thermal mass up to 300°C, a first-order approximation of a linear fit may be used in the molding temperatures from 300°C to 700°C. This linear fit of the structural stiffness as a function of temperature takes the following form:

$$SS(T) = (-88.9 \times 10^3)T + 142.5 \times 10^6, \quad (3)$$

where  $SS$  is the structural stiffness in N/m and  $T$  is the molding temperature in degrees Celsius. The slope constant has units of N/m  $\cdot$  °C, and the intercept constant has units of N/m. Equation (2) is used to help determine the position as a function of force in

$$P_a = P_r - \frac{F_a}{((-88.9 \times 10^3)T + 142.5 \times 10^3)}, \quad (4)$$

where  $P_a$  is the actual position and  $P_r$  is the recorded position of the LVDT measured in millimeters from the top home position. The force  $F_a$  is taken from (2). Scatter from the raw data as seen in Figure 4(a) was used for (5). Equation (5) shows an estimated relationship of the force and the error of position:

$$P_{\text{err}} = \pm (3 + 0.002F_a), \quad (5)$$

where  $P_{\text{err}}$  is the error of the position values and the constant 3 has units of microns while the constant 0.002 has units of microns per N. The temperature does not seem to have a statistically significant effect on the error of the position or the scatter in the stiffness data as a function of force. All of these information are important to understand prior to pressing in order to achieve the precision needed for the PGM for optical elements. The information can be used to determine an approximate baseline for an experiment and can simultaneously show where possible sample center thickness error could be arising. These findings ultimately will save time and money, as finding the optimal pressing positions will be less of an iterative process.



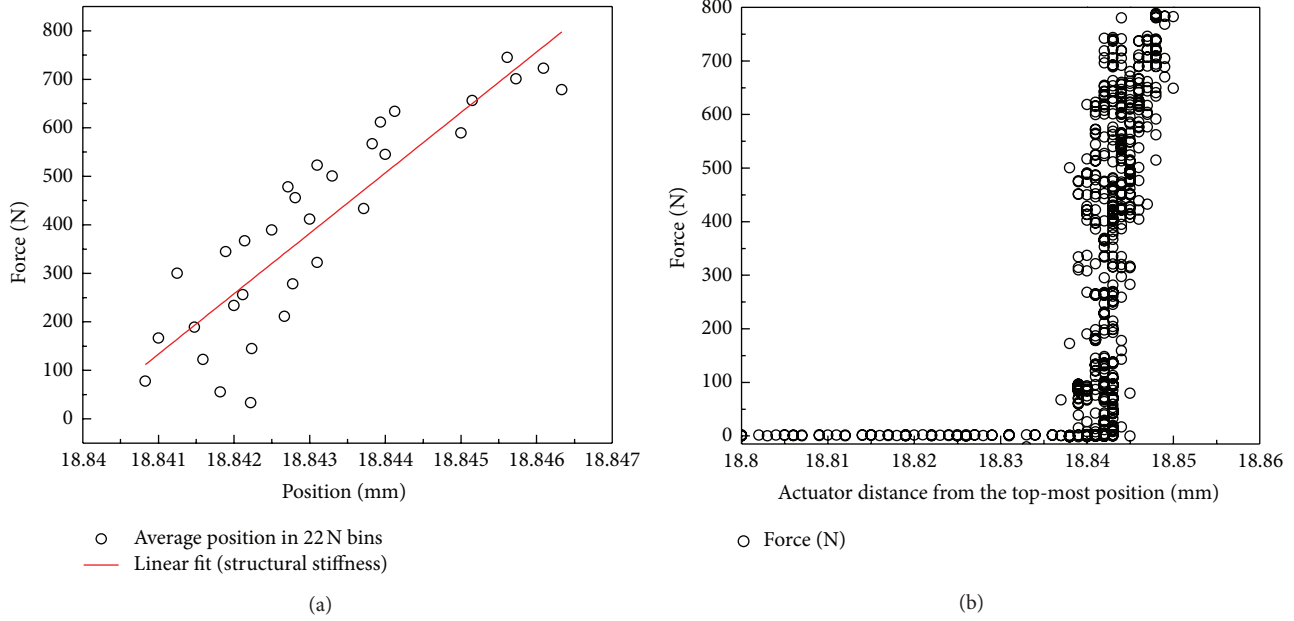


FIGURE 5: (a) An example of the raw data taken at room temperature for the structural stiffness experiments. (b) Analysis of the room temperature raw data for determining the structural stiffness using 22 N bin averages of position with a linear fit.

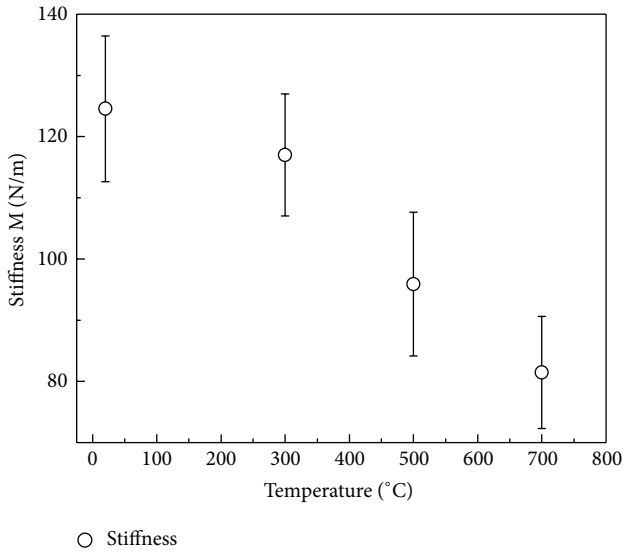


FIGURE 6: Structural stiffness of the GP500-HT as a function of temperature.

**2.5. Molding Cycle.** The molding cycle is comprised of several stages: purging, heating, soaking, molding, and cooling. The measurement devices embedded in the press drive the transition between these stages in the molding process. Before a cycle starts, the user programs the setpoints for a molding program. These setpoints are the triggers that cause the press to move to the next stage in the cycle. The user has two options for running a given pressing cycle: auto mode runs through a full cycle when the start button is pressed, and

manual mode gives the user control over when the different stages begin.

Figure 7 shows a typical molding cycle with temperature and force as a function of time. The stages of the pressing cycle are labeled.

Once the molding cycle is started, the upper molding chamber lowers and seals the molding chamber. The press is then evacuated using a vacuum pump and then backfilled with inert gas (nitrogen) three times in order to prevent oxidation of the molds and other components in the molding chamber. The evacuation pressure, back fill pressure, and number of cycles are user specified inputs.

Once purged, the soaking stage begins, and the actuator moves into the sleeve quickly to a user defined height above the position it will come into contact with the glass. The actuator continues to move from that point slowly until it comes into contact with the glass sample and applies a user-defined force. Once the soaking force is reached, the heaters heat either at full output until 95% of the target temperature where the PID values take over or at a user-defined ramp rate. Once the thermocouples near the molding surface reach the commanded temperature, the soak timer begins. The soak time can be as short as 1 second or extend for hours. The soak allows the glass sample to equilibrate at a uniform temperature to ensure the glass has a uniform viscosity. When the soak time has elapsed, the pressing stage begins. The pressing stage is force driven but position limited: the actuator begins to press the glass until a specified force is reached, and the actuator holds the pressing force until the final position is reached. The final press position is determined from the room temperature (RT) bottom position ( $P_{RT}$ ):

$$FPP = P_{RT} + CT_{Final} + \text{Baseline}, \quad (6)$$

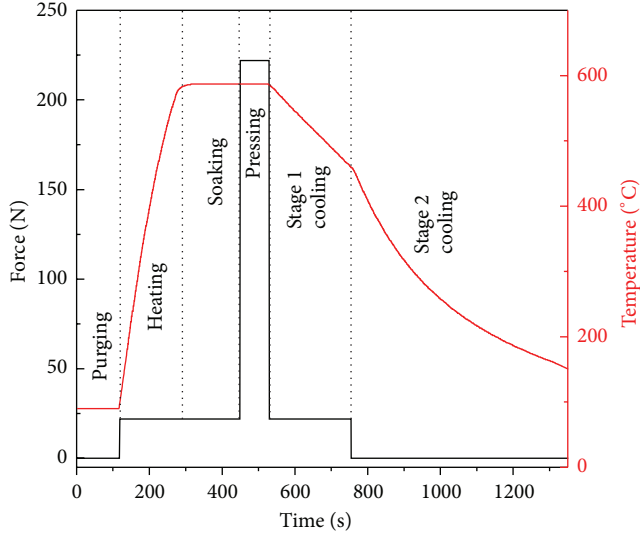


FIGURE 7: The molding cycle used for the repeatability tests in this study with temperature and force as a function of time.

where  $CT_{\text{Final}}$  is the desired final press part center thickness and the Baseline is determined by combining (1), (2), and (4). The full master equation for the FPP is

$$\begin{aligned} \text{FPP} = & P_{\text{RT}} - CT_{\text{Final}} \\ & - \frac{1}{1000} \left[ \left( A_1 e^{(-T_m/B_1)} + C_1 \right) e^{(-t/(A_2 e^{(-T_m/B_2)} + C_2))} \right. \\ & \left. + \left( A_3 e^{(-T_m/B_3)} + C_3 \right) \right] \\ & + \frac{F_r - (0.045T_m)}{((-88.9T_m) + 142.5 \times 10^3)}. \end{aligned} \quad (7)$$

The final pressing position is also a safety feature: regardless of the pressing stage or cycle, when the LVDT output reaches the final position, the cooling stage begins. The press can be cooled at the maximum cooling rate or using up to three separate cooling sections with control over the cooling rate and applied force. This cooling ramp control gives more control over the amount of stress remaining in the glass. The whole pressing cycle is completed when the press reaches a safe user-defined temperature; at that time, the upper mold chamber is raised, the lower chamber is slid out, and the upper tooling is removed. The molded glass sample can then be removed for analysis.

Auto-mode allows for full cycles to be complete under the set points, but to have more versatility on the segments of the molding cycle, the manual mode is needed. Manual mode allows the user to start and stop cycles at any time and gives full freedom of the actuator, the cooling, and can be used to find set points. Manual mode does not allow for 3 sections in the cooling stage but does give the flexibility of individually using the upper, lower, and chamber gas cooling. Manual mode also has an option to monitor the heaters power and temperature control during any stage of the molding cycle.

### 3. Repeatability Results

The goal of the repeatability measurements is to determine the ability of the press to produce similar results on a day-to-day basis and also on a per cycle basis. The target function for both of the data sets is the center thickness of the sample after it has been pressed.

**3.1. Methodology.** The samples used during the pressing cycles are square-cut plane parallel plate (PPP) windows of L-BAL35 glass from Ohara Inc., as this is a glass currently being used for molding in industrial settings. The glass's physical properties needed for PGM such as viscosity, glass transition temperature, viscoelastic response, and structural relaxation parameters are known for L-BAL35 [10]. Dimensionally, each PPP window square measures approximately 5 mm on a side, with a thickness of approximately 2 mm. The cycle parameter set points for this pressing cycle are listed in Table 4.

While in auto mode, the press heats the sample to 590°C and molds the sample with a force of 222 N. The sample is cooled in two stages, with different rates of cooling. A graphical representation of the molding cycle used for the repeatability is shown in Figure 7.

The data collected on the repeatability can be broken into two sets. The first data set includes only the data from the first cycle of the day. This data set is representative of the day-to-day variations exhibited by the instrument. The second set of tests includes data from all cycles, including the first-cycle-of-the-day data already presented in the first data set. The second data set mimics a typical production cycle used in industry [3]. Twelve consecutive pressing cycles were taken on three different days. The sample thickness was measured in 10 places to determine a mean value and standard deviation of the center thickness for each individual sample. In the 12 consecutive cycles there are two distinct phases in the press' repeatability. The first phase, or the "warm up" phase, includes the first 2–4 runs (shown in Figures 4(b) and 8), where the press experiences thermal expansion between pressing cycles. The second phase, referred to as the "steady state," includes all cycles after the warm-up phase, where the thermal expansion is constant between pressing cycles. The boundary line between the two phases is somewhat arbitrary but is distinguished by a significant drop in the standard deviation of the sample thickness across the three days.

**3.2. Results.** The individual measurements of each sample show that they have a highly uniform thickness, varying only a few microns with a maximum standard deviation of 2 microns as listed in Table 5.

Table 5 also shows the total range and the standard deviation of the first cycle and all of the steady state samples. A large difference exists in repeatability capabilities from the first cycle to the steady state; an order of magnitude drop of the standard deviation and the total range from the first cycle to the steady state cycles is shown. The steady state average center thickness is 1.001 mm, showing that the press can reach desired center thicknesses.

TABLE 4: Pressing parameters used in determining system repeatability.

	Cycle parameters
Purge limits (psi)	-12/2
Soak force (N)	22
Pressing temperature ( $^{\circ}\text{C}$ )	590
Soak time (min)	2
Pressing force (N)	222
Final position ( $\mu\text{m}$ from $P_{\text{RT}}$ )	1717
Cooling section 1 temperature ( $^{\circ}\text{C}$ )	590
Cooling section 1 ramp rate ( $^{\circ}\text{C}/\text{min}$ )	35
Cooling section 1 force (N)	22
Cooling section 2 temperature ( $^{\circ}\text{C}$ )	450
Cooling section 2 ramp rate ( $^{\circ}\text{C}/\text{min}$ )	None
Cooling section 2 force (N)	4
Chamber open temperature ( $^{\circ}\text{C}$ )	150

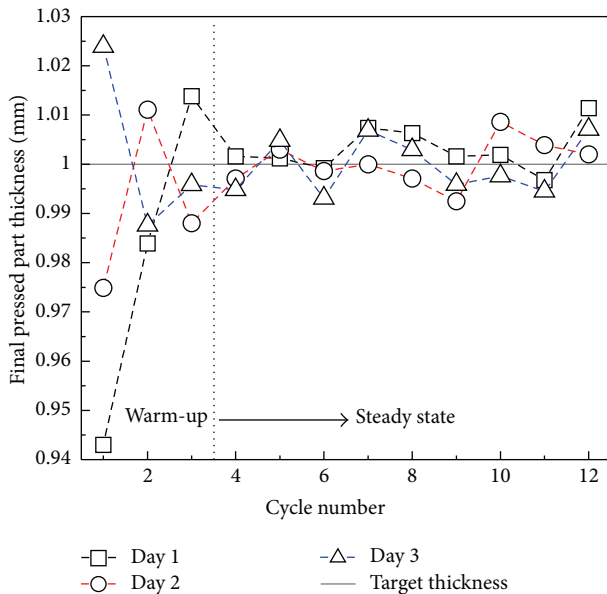


FIGURE 8: The center thicknesses of the final pressed part pieces through the cycle number over multiple days in 12 consecutive pressing cycles.

TABLE 5: The standard deviation and the total range of the thickness of an individual sample, the first molding cycle of the day, and the steady state.

	Individual samples	First cycle	Steady state
Standard deviation ( $\mu\text{m}$ )	2	81	5.5
Total range ( $\mu\text{m}$ )	6	41	21

Within the whole data set, the effect of thermal expansion on the target function can be analyzed. These results show several machine tool attributes that would be important to a lens manufacturer: the uniformity of the pressed part

thicknesses and how quickly (how many pressing cycles) before this uniformity can be obtained. As the press transitions from room temperature through the warm-up phase, the average thickness of the resulting samples continually changes. However, once the press has reached its “steady-state phase,” the thicknesses of the pressed pieces remain essentially constant. Comparing the deviation from the target thickness of each numbered cycle, from 1 to 12, over 3 consecutive days of cycles, a definite trend is evident, and is shown in Figure 8. As the number of cycles increases past the third cycle of that day, the standard deviation of the sample thickness decreases.

Figure 8 shows the actual center thicknesses of the pieces run over three different days. There is a drastic difference in the error of the center thicknesses after 3 cycles, once again showing the warm-up period of the press. The standard deviation of the thickness of the individual samples is within the data points.

Errors in the pressed part can be traced to three factors in the experiment: the cycle-to-cycle mechanical movement, the thermal mass cycling, and the actual part being pressed. The error of the final pressed part can be shown to come from three aspects of molding: mechanical, thermal, and the press material. The cycle-to-cycle mechanical movement shows a  $1.8 \mu\text{m}$  error. The error recorded from the thermal mass cycling was as high as  $4 \mu\text{m}$ . With  $1.8 \mu\text{m}$  error coming just from the mechanical movement of the system,  $2.2 \mu\text{m}$  error comes from that actual thermal cycling. By introducing the sample and the full molding cycle, the error is  $5 \mu\text{m}$ . This means the error from the sample and the entire molding cycle contribution is a  $1 \mu\text{m}$  addition to standard deviation of the total error.

## 4. Conclusions

A commercially available, bench-top precision glass molding machine is a valuable tool for research in the demanding and growing optoelectronic industry and scientific field. Based on experience in our facility, it has been found to be a tool that can help bridge the difficult and important gap between scientific research and industrial manufacturing. The GP-5000HT is a glass molding machine with functionality similar to a full-production molding machine but is also versatile enough to be used for scientific research purposes.

A steady-state baseline was shown to be needed due to pressing cycle setpoints being position limited, and the systems position was found to be a function of the temperature, time at temperature, and force; this finding demonstrates one of the reasons why molding is still an iterative process. A master baseline was created for this press to account for the system position change. The baseline proved to be predictive and valid for a standalone test of temperature, time, and force. Furthermore, the master baseline was found to be valid for the repeatability tests.

Preliminary repeatability results utilizing pressed part thickness of plano-plano samples have shown an increase in thickness consistency across a number of days as the number of molding cycles increases. There is still a large uncertainty

to the first cycle results and that there is a definite “warm-up” period, though industry routinely runs “dry” cycles, without glass, over some defined period. The tolerances of the final thickness become much tighter after the system reaches thermal equilibrium, typically after 3 molding cycles. During the steady state cycles done over multiple days, the total range of thicknesses is 21  $\mu\text{m}$  with a standard deviation of 5  $\mu\text{m}$ . The systematic study of the system has also shown that about 36% of the error comes from the mechanical movement from cycle to cycle, 44% comes from repeatability of thermal mass from cycle to cycle, and 20% comes from the introduction of the sample in the system.

This study has shown that the DTI GP5000-HT is capable of routine future tests (daily, weekly, etc.) with target boundaries and final piece tolerances that can also be developed from this set to ensure the press is performing within acceptable limits of operation.

## References

- [1] Nanotechsys.com, *New Hampshire*, Moore Nanotechnologies LLC., 2010, <http://www.nanotechsys.com/machines/nanotech-gpm-glass-press-molding/>.
- [2] Toshiba-machine.co.jp, Toshiba Machine Co. LTD., Tokyo, Japan, 2010, <http://www.toshiba-machine.co.jp/english/product/high/contents/molding.html>.
- [3] Private communication with industrial partners.
- [4] Dti-fla.com, Dyna Technologies, Inc., Sanford, Fla, USA, 2010, <http://dti-fla.com/glassmolding.html>.
- [5] K. D. Fischbach, K. Georgiadis, F. Wang et al., “Investigation of the effects of process parameters on the glass-to-mold sticking force during precision glass molding,” *Surface and Coatings Technology*, vol. 205, no. 2, pp. 312–319, 2010.
- [6] D. H. Cha, H. J. Kim, H. S. Park et al., “Effect of temperature on the molding of chalcogenide glass lenses for infrared imaging applications,” *Applied Optics*, vol. 49, no. 9, pp. 1607–1613, 2010.
- [7] S. Gaylord, B. Ananthasayanam, B. Tincher et al., “Thermal and structural property characterization of commercially moldable glasses,” *Journal of the American Ceramic Society*, vol. 93, no. 8, pp. 2207–2214, 2010.
- [8] P. Mosaddegh, *Friction measurement in precision glass molding [Dissertation]*, Clemson University, Clemson, Mich, USA, 2010.
- [9] Y. A. Cengel, *Heat Transfer—A Practical Approach*, McGraw Hill, New York, NY, USA, 2003.
- [10] S. Gaylord, *Thermal and structural properties of candidate moldable glass types [Dissertation]*, Clemson University, Clemson, Mich, USA, 2008.